Catalysis Science & Technology

Accepted Manuscript

ROYAL SOCIETY OF CHEMISTRY

www.rsc.org/catalysis

Journal Name

RSC Publishing

ARTICLE

Barium zirconate: a new photocatalyst for converting CO_2 into hydrocarbons under UV irradiation

Cite this: DOI: 10.1039/x0xx00000x

Xianliu Chen [a], Jun Wang [a], Chunxiang Huang [a], Shiying Zhang [b], Haitao Zhang [c], Zhaosheng Li [a],* Zhigang Zou [a]

Received ooth January 2012,
Accepted ooth January 2012

DOI: 10.1039/x0xx00000x

www.rsc.org/

In this study, photocatalytic activities of $BaZrO_3$ for CO_2 reduction were investigated in detail. $BaZrO_3$ samples were successfully obtained via a Pechini process at different temperatures. The prepared samples were characterized by X-ray diffraction (XRD), BET surface area measurement, UV-vis absorption spectra, scanning electron microscopy (SEM) and transmission electron microscopy (TEM). The effects of the deposition of various metal nanoparticles on the surface of $BaZrO_3$ were also discussed. The results proved that the highly dispersed silver nanoparticles play a crucial role on the photocatalytic activities of $BaZrO_3$.

1. Introduction

Nowadays with the depletion of the unrenewable fossil fuels and the rising atmospheric levels of carbon dioxide, environmental pollution and the greenhouse effect becomes more obvious, which raise the increasing concerns about the ensuing crisis of the energy supply and the global climate. Also , CO_2 is supposed to be the most important greenhouse gas [1,2]. An ideal way to cut down the increasing atmospheric levels of CO_2 and relieve the crisis of fossil energy simultaneously is to convert CO_2 into hydrocarbons under the solar irradiation. However, CO_2 could not absorb the irradiation in the wavelength 200-900 nm, indicating that the photoreduction of CO_2 requires suitable photosensitizers. Both the metal complexes and semiconductors have been utilized to absorb visible/UV irradiation and transfer this energy to CO_2 [3]. Since CO_2 can be photoreduced into hydrocarbons under UV light at room temperature and ambient pressure [4], applying the photocatalyst with cocatalyst is also a promising way to efficiently solve the problems mentioned above [5-7].

To date, TiO_2-based photocatalysts have been developed extensively for CO_2 photoreduction [8-15]. Recently, other photocatalysts such as $ZnGa_2O_4$ [2], Zn_2GeO_4 [16], $NaNbO_3$ [17], Bi_2WO_6 [18] and $BaLa_4Ti_4O_{15}$ [19] have been studied for photo-reduction of CO_2 into hydrocarbons. The development of new photocatalysts for CO_2 conversion could enhance our understanding of this photoreduction process [20].

$BaZrO_3$ has been extensively studied for over ten years [21,22]. Due to its small thermal expansion coefficient, poor thermal conductivity, good mechanical properties, thermal stability and low chemical reactivity towards corrosive compounds, it has been investigated in various applications, such as thermal barrier coating material in airspace industry, a good substrate for the manufacturing for high temperature superconductors[23] and material for interface engineering of alumina fiber-alumina matrix composites [24,25]. Pure $BaZrO_3$ has been also proved to be an efficient photocatalyst for water splitting under the UV light irradiation. For the cubic perovskite structure $BaZrO_3$ with 180° Zr-O-Zr bond angle, the photogenerated electrons and holes in $BaZrO_3$ should be easy to delocalize and transfer to the surface [26]. The evolution rate of H_2 was 522.0 μ mol·h^{-1}·g^{-1}, which was significantly higher than that of the pure anatase TiO_2 powders [26].

The DFT (density functional theory) calculation results of $BaZrO_3$ show that the top of the VB is contributed by O 2p orbitals, while the bottom of the CB is dominated by Zr 4d orbitals. Besides, the top of the VB and the bottom of the CB locate at the R point and the G point, respectively, which indicate that $BaZrO_3$ is an indirect-gap semiconductor [27]. The calculated band gap (3.2 eV) is smaller than that of experiment value (4.8 eV). The bottom of the CB and the top of the VB of $BaZrO_3$ locates at -1.8 eV and 3.0 eV versus NHE, pH 7.0, respectively. The photogenerated electrons in the CB are more negative than the potential of CH_4/CO_2, CH_3OH/CO_2,

$HCHO/CO_2$ and $HCOOH/CO_2$ redox couples. The corresponded holes in the VB are easy to oxidize H_2O. Then the energy of the photogenerated electrons and holes should be sufficient for CO_2 photoreduction using water as a reducing agent under UV irradiation. But the width of its band gap severely restricts the absorption of light [28].

To the best of our knowledge, no results have been reported about the photocatalytic activity of $BaZrO_3$ for CO_2 reduction under UV light irradiation. Furthermore, it is important to investigate the photocatalytic activity of $BaZrO_3$ with the assistance of cocatalysts. In this study, a series of $BaZrO_3$ samples were synthesized by the pechini technique and characterized by X-ray diffraction, BET surface area, UV-vis diffuse reflectance spectra, SEM and TEM. And the photocatalytic activities of $BaZrO_3$ with various cocatalysts loaded in CO_2 reduction under UV irradiation have been investigated in detail.

2. Experimental

2.1 Sample synthesis

The $BaZrO_3$ samples were prepared as that reported by our previous paper [26]. Stoichiometric amounts of $Zr(NO_3)_4 \cdot 5H_2O$ and $Ba(NO_3)_2$ (both are analytical reagent grade) were initially prepared in a beaker. Then，a mixture of 60 wt% citric acid monohydrate ($C_6H_8O_7$, purity ≥99.9%) and 40 wt% ethylene glycol ($C_2H_6O_2$, purity ≥99.9%) (the molar ratio of citric acid to total cations was fixed at 2:1) was added into the beaker. Subsequently a solution was acquired by adding distilled water into the beaker. This solution was homogenized by stirring at room temperature for about 1 h. Then the prepared clear solution was evaporated in bake oven at 343 K until a brown resin was formed. The obtained resin was heated for 6 h at 673 K to remove the majority of the organics. After that, the obtained solid was ground using agate mortar, and finally thermally sintered at different temperatures (1173, 1273, 1373, 1473 K) for 10 h in air atmosphere.

Noble metals (Ag, Au, Pt) were deposited on the surface of $BaZrO_3$ as the different cocatalysts through liquid phase chemical reduction according to reported method [19]. Cation solution ($AgNO_3$, $HAuCl_4$, H_2PtCl_6) of 0.1 mol/L of was added to 30 ml of an aqueous suspension containing 0.2 g $BaZrO_3$. After adding an equimolar amount of NaH_2PO_2 (0.4 mol/L) with respect to cation in the suspension, the mixture was stirred at 333 K for 1 h. The obtained mixture was washed with distilled water and dried at 343 K in air. Then the sample was annealed at 573 K for 1 h [29].

The deposition of Cu and Ru cocatalyst were carried out via an impregnation method. The corresponding cation solution ($CuCl_2$, $(NH_4)_2RuCl_6$) and calcinations at 723 K for 1 h were selected as the condition of the impregnation method. The reduction treatment was carried out under H_2 gas flow at 573 K for 2 h.

2.2 Characterization

The data of the crystal structure and the phase purity were collected by a powder X-ray diffractometer (Ultima Ⅲ, Rigaku, Japan) using Cu Kα radiation. The acceleration voltage was 40kV, and the emission current was 40 mA. The diffractograms were recorded in the 2θ rang from 20^o to 80^o at a scan rate of 10^o/min. The UV-vis reflectance spectra were recorded with a UV-vis spectrophotometer (UV-2550, Shimadzu, Japan) using $BaSO_4$ as the background. The specific surface area of the $BaZrO_3$ samples was determined by BET measurement (TriStar-3000, Micromeritics, USA) of nitrogen adsorption at 77 K. Transmission electron microscopy (JEOL 3010) was employed to characterize the surface morphologies of $BaZrO_3$ powder and silver nanoparticles. The gas products were detected by gas chromatograph with double-FID (GC-2014, Shimadzu, Japan).

2.3 Photocatalytic experiments

The photocatalytic reaction was executed in a cylindrical quartz cell. A plate glass loader filled with fresh sample (0.1g) was located in the cell. The reaction system was connected with a traditional vacuum system and stabilized at ambient temperature by flowing cool water. After the sample was loaded, the reaction system was evacuated to about 1mTorr using a mechanical pump and then sealed. Carbon dioxide (99.99% pure) was transmitted into the reaction system until the pressure reached 93.5 kPa. Before adding 0.4 ml distilled water into the reaction system, the distilled water was heated at 100 ^oC in order to drive out the dissolved O_2. Then, the sample absorbed CO_2 and water vapor for 8 h in dark with the gas circulator working. Before the illumination, 1 ml gas sample was withdrawn and injected into gas chromatograph by a gas-tight syringe (1 ml) and the analysis was used as the reference.

In the experiments, 300W Xe lamp (PE 300BUV) was used as the light source. The whole reaction system was tightly closed during the irradiation. According to the analysis of the gas chromatograph, methane was the major hydrocarbon in all these experiments. Therefore, the direct measure of activity toward CO_2 photoreduction was referenced to the methane yield. To make sure the hydrocarbon products were attributed to the photoreduction of CO_2, three contrast tests were carried out. The first one was UV-illuminated without the catalyst, the second one was the dark reaction under the same experimental conditions and the third one was that illuminated photocatalyst in the absence of CO_2. All the reactions have been repeated more than five times to confirm the reproducibility and consistency of the photocatalytic experiment.

3. Results and discussion

3.1 Characterization

The crystal structures of the samples prepared from 1173 to 1473 K were detected by XRD measurement, as shown in Fig 1. The sample prepared at higher temperature showed higher intensity and narrower diffraction peaks, indicating the improvement of the crystallinity. For the sample prepared at

1173 K, the XRD diffraction patterns of $BaCO_3$ could be found, which should be contributed to the relatively low calcination temperature in the synthesis process. According to the XRD patterns, the lattice parameter of $BaZrO_3$ prepared at 1273 K could be calculated as 4.18Å, which is consisted with other report [30]. Pure $BaZrO_3$ could also be obtained via the solid state reaction at relative high temperature about 1873 K [31].

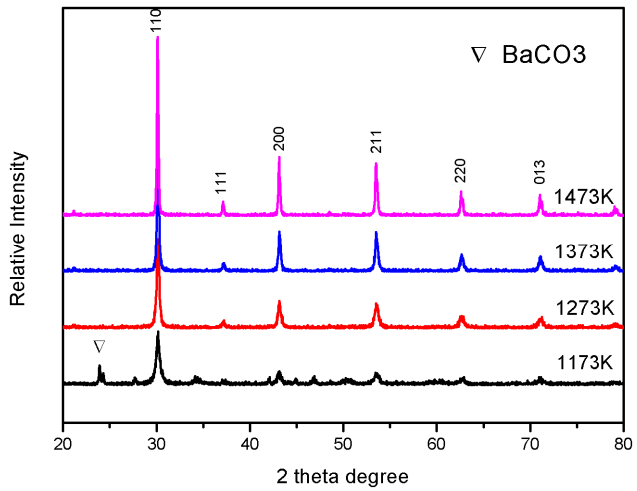

Fig. 1. XRD patterns of $BaZrO_3$ synthesized at 1173, 1273, 1373 and 1473 K

The UV-vis and BET surface data have been acquired. The specific surface area of $BaZrO_3$ obtained at 1273 K was 2.30 m^2/g. And the absorption edge of $BaZrO_3$ located at about 260 nm, which indicates $BaZrO_3$ is a wide-band gap semiconductor. The band gap of $BaZrO_3$ is estimated to be 4.8 eV, which is obtained by processing the UV-vis spectra data of $BaZrO_3$ with the Kubelka-Munk method. The calculated band gap of $BaZrO_3$ has been reported as 3.2 eV [26], which is less than the experimental value, due to one electron approximation.

Just as depicted in Fig 2, no hydrocarbons were detected in the above blank experiments. The three blank reactions illustrated that both the photocatalyst and the light irradiation were indispensable for the CO_2 photoreduction process. Fig. 2 also depicts the CH_4 production amount from the above photocatalytic system containing different photocatalysts prepared at different temperature under UV-light irradiation for 8 h. It could be found that, the $BaZrO_3$ samples prepared at different temperature show similar photoreduction activity. All the $BaZrO_3$ samples showed relative low photocatalytic activity, which should be ascribed to the low BET surface and the low efficiency of the electron–holes separation. The experimental results also showed that CH_4 was the primary product in the gaseous photocatalytic CO_2 reduction system by using $BaZrO_3$ as photocatalyst. The selective formation of CH_4 rather than other hydrocarbons (such as CH_3OH and CO) might be attributed to that the redox potential of CH_4/CO_2 [$E^0(CH_4/CO_2)$=-0.24V versus NHE, pH=7.00] is much lower than that of CO/CO_2 [$E^0(CO/CO_2)$=-0.53V versus NHE, pH=7.00] or CH_3OH/CO_2 [$E^0(CH_3OH/CO_2)$= -0.38V versus NHE, pH=7.00] [32,33].

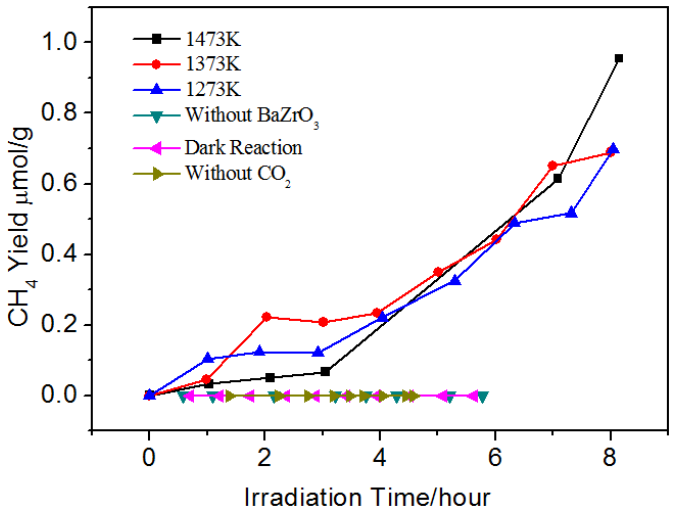

Fig.2. The products were detected in three blank reactions and the CH_4 yield of pure $BaZrO_3$ prepared at different temperatures (1273, 1373 and 1473K).

To confirm the effect of the cocatalyst on the photocatalytic activities, various noble metals particles were deposited on the surface of $BaZrO_3$ prepared at 1273 K. Au, Pt, and Ag nanoparticles were obtained by the liquid chemical reduction method, while the Cu and Ru particles were prepared by an impregnation method. The CH_4 evolution rate over the $BaZrO_3$ samples with different cocatalyst deposited ($BaZrO_3$-0.5wt% Pt, $BaZrO_3$-0.5wt% Ag, $BaZrO_3$-0.5wt% Cu, $BaZrO_3$-0.5wt% Au, $BaZrO_3$-0.5wt% Ru) under illumination for 6 hours were shown in Fig. 3.

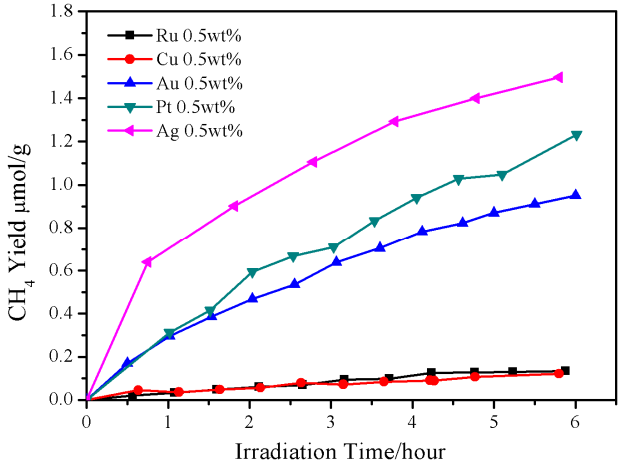

Fig. 3. The CH_4 yield of $BaZrO_3$ deposited by different cocatalysts (Ru, Cu, Au, Pt, Ag) with the same appearent amount.

According to the results shown in Fig 3, three samples ($BaZrO_3$-0.5wt% Pt, $BaZrO_3$-0.5wt% Ag, $BaZrO_3$-0.5wt% Au) exhibited higher photoactivity than the pure $BaZrO_3$ (1273 K) shown in Fig. 2, whereas the other two samples ($BaZrO_3$-0.5wt% Cu, $BaZrO_3$-0.5wt% Ru) showed much lower photoactivity than that of the pure $BaZrO_3$. And the sample $BaZrO_3$-0.5wt% Ag exhibited the highest photocatalytic efficiency. The coverage and adsorption of CO_2 may be more

feasible to carry out on the surface of $BaZrO_3$-0.5wt%Ag, which would result in the better photoreduction activity in contrast with the other samples. To find the optimal deposition amount of Ag nanoparticles, $BaZrO_3$ samples with various weight ratio of Ag (0.5 wt%, 0.3 wt%, 0.1 wt%) deposited were chosen for further investigation, and the results were shown in Fig. 4.

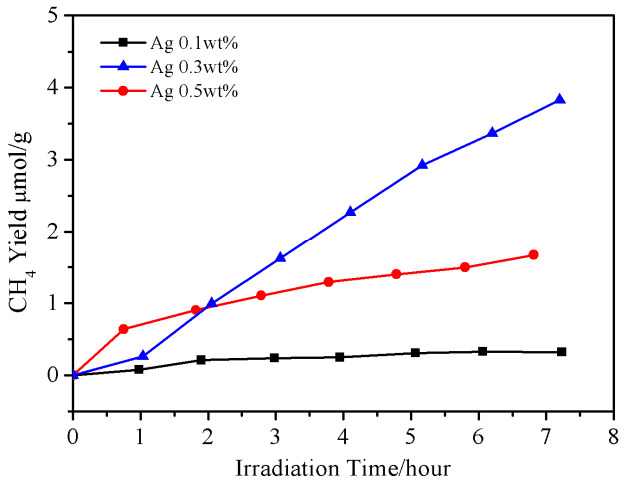

Fig.4. The CH_4 yield of $BaZrO_3$ with different amount Ag deposition.

The Ag deposition can increase the methane yield owing to the increasing amount of active sites. As shown in Fig 4, $BaZrO_3$-0.3wt% Ag showed higher photoactivity than that of $BaZrO_3$-0.1wt% Ag. The $BaZrO_3$-0.5wt% Ag sample exhibited relative lower photoactivity than that of $BaZrO_3$-0.3wt% Ag, which should be contributed to the excess Ag deposition covered up the surface of $BaZrO_3$ and hampered the light absorption, depressing the photogenerated e^--h^+ separation efficiency.

The $BaZrO_3$ powder with 0.3wt% Ag deposited was investigated by SEM, TEM and HRTEM (Fig 5). The Ag nanoparticles could be found from the SEM microphotograph as shown in Fig 5(a). The TEM image in Fig 5(b) clearly displayed that the silver nanoparticles aggregates on $BaZrO_3$ surface with an average size of about 5nm, which was agreed with the report before [19]. The enlarged high resolution transmission electron microscopy (HRTEM) image of the selected area (Fig 5(c)) exhibited well-defined lattice fringes with an interplanar spacing of 0.29 nm corresponding to (110) plane of $BaZrO_3$. And the adjacent lattice fringes were also consisted of the lattice spacing of 0.24 nm which was coincided with the (111) plane of silver. The continuity of lattice fringes between $BaZrO_3$ and Ag verified the formation of Schottky barrier between them. Under the observed projections, other particles with diameter of about 15nm were found on the edge of $BaZrO_3$ particles. Since their sizes were much smaller than that of $BaZrO_3$, it may be contributed to the excessive aggregate of the silver particles. The SEM, TEM and HRTEM images proved that silver nanopaticles dispersed on the surface of the $BaZrO_3$ surface uniformly. These silver nanoparticles changed at the beginning stage of the photocatalytic reduction which result in the increase of the photocatalytic activities [19].

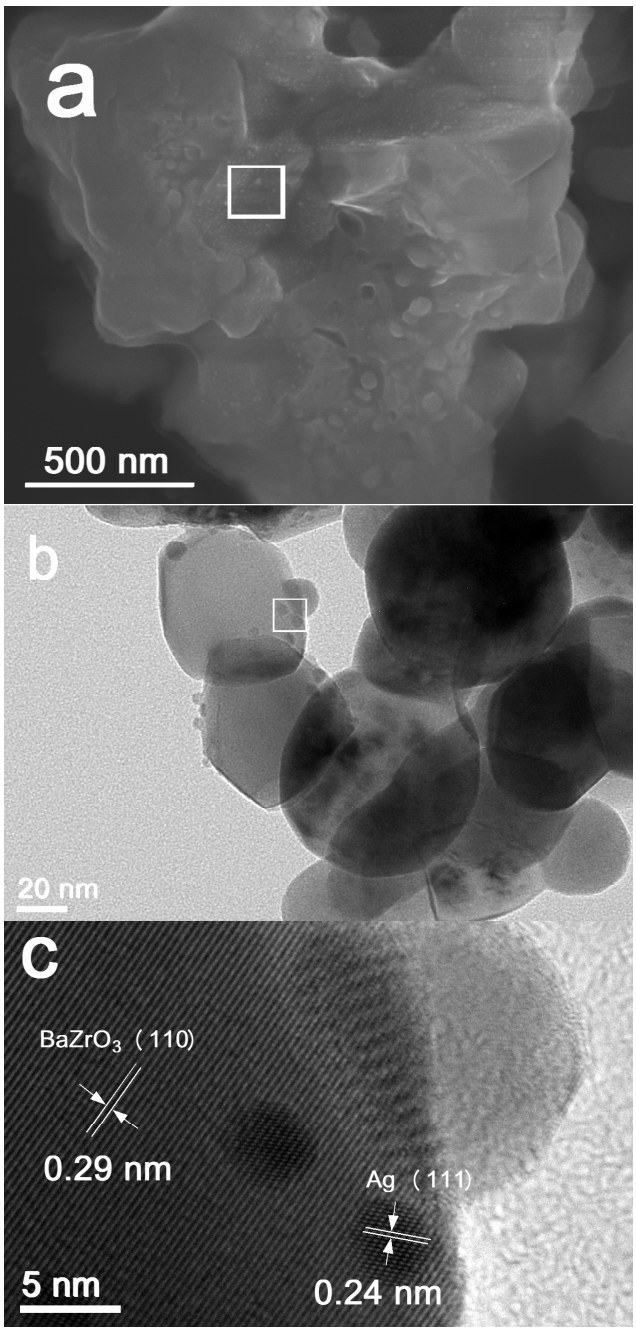

Fig.5. (a) SEM microphotograph of $BaZrO_3$ deposited by 0.3wt% Ag. (b) TEM pattern and (c) HRTEM pattern of 0.3wt% Ag deposited $BaZrO_3$.

Under UV light irradiation, the electrons in the valence band (VB) are excited by the photon to the conduction band (CB). And the CO_2 or intermediate molecules adsorbed on the surface of $BaZrO_3$ could be reduced by the photogenerated electrons. Due to the large band gap of $BaZrO_3$, the utilization of the irradiation light is limited, which may lead to relative low photocatalytic activity. However, the deposition of silver on the surface of $BaZrO_3$ enhanced the photocatalytic efficiency. In the case of silver deposited $BaZrO_3$, the photogenerated

electrons are trapped by silver nanoparticles under UV light, which leads to a better interfacial charge transfer and a sharply decrease in the recombination rate. This is attributed to that its E_F level is lower than the CB of $BaZrO_3$ [34]. When this semiconductor-metal composite are exposed to UV light, the photogenerated electrons in $BaZrO_3$ transfer to silver nanoparticles and this continues until they attain equilibrium, which shifts the Fermi level of the semiconductor-metal composite upward and increases the negative potential of silver [34,35]. This negative shift in E_F leads to better charge separation and more reductive power for the catalyst system. At the interface of silver and $BaZrO_3$, a Schottky barrier is formed, which would promote the separation of the charge carriers through accumulating electrons into silver and remaining holes back in $BaZrO_3$ [3, 36-39].

4. Conclusions

The photocatalytic properties of $BaZrO_3$ have been investigated as a new photocatalyst for CO_2 reduction. The $BaZrO_3$ samples obtained at 1273K with 0.3wt% Ag nanoparticles deposited showed the highest photocatalytic activities. Under UV light irradiation, the Ag nanoparticles deposited $BaZrO_3$ showed higher photocatalytic activities than the samples with other metal nanoparticles deposited. The Ag nanoparticles dispersed on $BaZrO_3$ results in more efficient separation of the photogenerated electron-hole-pairs, and the electron transmission mechanism should be further investigated in detail to enhance the photocatalytic activity of $BaZrO_3$.

Acknowledgements

This work is supported by National Basic Research Program of China (973 Program, 2013CB632404), a Project Funded by the Priority Academic Program Development of Jiangsu Higher Education Institutions, New Century Excellent Talents in University (NCET-12-0268), the National Natural Science Foundation of China (Nos. 51272102 and 21103070) , and the Open Research Fund of Hunan Key Laboratory of Applied Environmental Photocatalysis (ccsu-KF-1404), Changsa University.

Notes and references

[1] S. C. Yan, J. J. Wang, H. Gao, N.Y. Wang, H. Yu, Z. S. Li, Y. Zhou and Z. G. Zou, Adv. Funct. Mater., 2013, 23, 758.
[2] S. C. Yan, S. X. Ouyang, J. Gao, M. Yang, J.Y. Feng, X. X. Fan, L. J. Wan, Z. S. Li, J. H. Ye, Y. Zhou and Z. G. Zou, Angew. Chem. Int. Ed., 2010, 49, 6400.
[3] S. N. Habisreutinger, L. Schmidt-Mende and J. K. Stolarczyk, Angew. Chem. Int. Ed., 2013, 52, 7372.
[4] M. Anpo, H. Yamashita, Y. Ichihashi and S. Ehara, J. Electroanal. Chem., 1995, 396, 21.
[5] E. J. Maginn, J. Phys. Chem. Lett., 2010, 1, 3478.
[6] P. Usubharatana, D. McMartin, A. Veawab and P. Tontiwachwuthikul, Ind. Eng. Chem. Res., 2006, 45, 2558.
[7] F. Sastre, A. V. Puga, L. C. Liu, A. Corma and H. García, J. Am. Chem. Soc., 2014, 136, 6798-6801.
[8] O.K. Varghese, M. Paulose, T.J. LaTempa and C.A. Grimes, Nano Lett., 2009, 9, 731.
[9] L. S. Yoong, F. K. Chong and B. K. Dutta, Energy, 2009, 34, 1652.
[10] K. Koci, L. Obalova, L. Matejova, D. Placha, Z. Lacny, J. Jirkovsky and O. Solcova, Appl. Catal. B: Environ., 2009, 89, 494.
[11] C. J. Wang, R. L. Thompson, J. Baltrus and C. Matranga, J. Phys. Chem. Lett., 2010, 1, 48.
[12]J. G. Yu, J. X. Low, W. Xiao, P. Zhou and M. Jaroniec, J. Am. Chem. Soc., 2014, 136, 8839−8842.
[13] J. Mao, K. Li and T. Y. Peng, Catalysis Science & Technology, 2013, 3, 2481-2498.
[14] A. Dhakshinamoorthy, S. Navalon, A. Corma and H. Garcia, Energy Environ. Sci., 2012, 5, 9217.
[15] Y. G. Wang, B. Li, C. L. Zhang, L. F. Cui, S. F. Kang, X. Li and L. H. Zhou, Appl. Catal. B: Environ., 2013, 130 − 131, 277 − 284.
[16] Q. Liu, Y. Zhou, J. H. Kou, X. Y. Chen, Z. P. Tian, J. Gao, S. C. Yan and Z. G. Zou, J. Am. Chem. Soc., 2010, 132, 14385.
[17] H. Shi, T. Wang, J. Chen, C. Zhu, J. H. Ye and Z. G. Zou, Catal. Lett., 2011, 141, 525.
[18] Y. Zhou, Z. P. Tian, Z. Y. Zhao, Q. Liu, J. Kou, X. Y. Chen. J. Gao, S. C. Yan and Z. G. Zou, Appl. Mater. Interfaces, 2011, 3, 3594.
[19] K. Iizuka, T. Wato, Y. Miseki, K. Saito and A. Kudo, J. Am. Chem. Soc., 2011, 133, 20863.
[20] S. C. Yan, J. J. Wang, H. L. Gao, N. Y. Wang, H. Yu, Z. S. Li, Y. Zhou and Z. G. Zou, Adv. Funct. Mater., 2013, 23, 1839.
[21] S. Jans, P. Wurz, R. Schletti, K. BrÜning, K. Sekar, W. Heiland, J. Quinn and R.E. Leuchtner, Nucl. Instr. Meth. in Phys. Res. B., 2001, 173, 503.
[22] J. Robertson, J. Vac. Sci. Technol. B, 2000, 18, 3.
[23] L. MacManus-Driscoll, S.R. Foltyn, Q.X. Jia, H. Wang, A. Serquis, L. Civale, B. Maiorov, M.E. Hawley, M.P. Maley and D. E. Peterson, Nat. Mater., 2004, 3, 439.
[24] A. Erb, E. Walker, R. Flukiger, Phys. C, 1995, 245, 245-51.
[25] S. Yamanakaa, M. Fujikanea, T. Hamaguchia, H. Mutaa, T. Oyamaa, T. Matsudab, S. Kobayashib and K. Kurosakia, J. Alloys Compd., 2003, 359, 109.
[26] Y. Yuan, X. Zhang, L. Liu, X. Jiang, J. Lv, Z. S. Li and Z. G. Zou, Int. J. Hydrogen Energy, 2008, 33, 5941-5946.
[27] P.W. Peacock and J. Robertson, J. Appl. Phys., 2002, 92, 4712.
[28] C. Lo, C. Hung, C. Yuan and J. Wua, Solar Energy Materials & Solar Cells, 2007, 91, 1765.
[29]R. Su, R. Tiruvalam, Q. He, N. Dimitratos, L. Kesavan, C. Hammond, J.A. Lopez-Sanchez, R. Bechstein, C.J. Kiely and G. J. Hutchings, ACS Nano, 2012, 6, 6284.
[30]Y. Hinatsu. J. Solid State Chem., 1996, 122, 384.
[31]L. Dong, D.S. Stone and R.S. Lakes, J. Mater. Res., 2011, 26, 1446.

[32]W.N. Wang, W.J. An, B. Ramalingam, S. Mukherjee, D.M. Niedzwiedzki, S. Gangopadhyay and P. Biswas, J. Am. Chem. Soc., 2012, 134, 11276-11281.
[33]V.P. Indrakanti, J.D. Kubicki and H.H. Schobert, Energy Environ. Sci., 2009, 2, 745–758.
[34]M. Jakob, H. Levanon and P.V. Kamat, Nano Lett., 2003, 3, 353–358.
[35]P. V. Kamat, J. Phys. Chem. Lett., 2012, 3, 663–672.
[36]V. Subramanian, E.E. Wolf and P.V. Kamat, J. Am. Chem. Soc., 2004, 126, 4943.
[37] M. Jakob, H. Levanon and P.V. Kamat, Nano Lett., 2003, 3, 353.
[38] S.T. Kochuveedu, Y.H. Jang and D.H. Kim, Chem. Soc. Rev., 2013, 42, 8467.
[39] S. Kim, S.J. Hwang and W. Choi, J. Phys. Chem. B, 2005, 109, 24260–24267.

a National Laboratory of Solid State Microstructures, Collaborative Innovation Center of Advanced Microstructures, College of Engineering and Applied Science, Ecomaterials and Renewable Energy Research Center, Nanjing University, No. 22 Hankou Road, Nanjing 210093, People's Republic of China.
b Hunan Key Laboratory of Applied Environmental Photocatalysis, Changsa University, Changsa, People's Republic of China
c School of Chemistry and Chemical Engineering, University of Jinan, Jinan, People's Republic of China
*Corresponding author. E-mail addresses: zsli@nju.edu.cn

